Supplemental Information

Efficient hydrogen isotope separation utilizing photocatalytic capability

Linzhen Wu[1], Sifan Zeng[1], Weiwei Wang, Shengtai Zhang, Hongbo Li*, Xiaosong Zhou*

Institute of Nuclear Physics and Chemistry, China Academy of Engineering Physics, Mianyang, 621900, China.

*. Corresponding author, E-mail address: **1234lihongbo@163.com** (Hongbo Li); zlxs77@126.com (Xiaosong Zhou)

[1]. These authors made equal contributions.

The calculation equation of the ratio of deuterium and hydrogen were deduced as follows:

Based on the linear relationship between the composition of individual gases and the response of the TCD, the concentration of individual gases can be obtained through

$$H_{gas} = \left(\frac{S_{H_2}}{f_x} \times 2\right) + \left(\frac{S_{HD}}{f_x} \times 1\right) = H_2 \times 2 + HD \quad \text{(S1)}$$

$$D_{gas} = \left(\frac{S_{D_2}}{f_x} \times 2\right) + \left(\frac{S_{HD}}{f_x} \times 1\right) = D_2 \times 2 + HD \quad \text{(S2)}$$

Where S_x(x=H_2, HD and D_2) is the peak area of individual gases and f_x is the coefficient between the gas peak area and the content analyzed by gas chromatography.

The ratio of deuterium and hydrogen is approximately:

$$\alpha_{H/D} = \frac{n_t}{n_0} = \frac{H_{gas}/D_{gas}}{H_{liq}/D_{liq}} = \frac{D_{liq} \cdot H_{gas}}{D_{gas} \cdot H_{liq}} = \left(D_{liq} \cdot H_{gas}\right) \big/ \left(D_{gas} \cdot H_{liq}\right) \quad \text{(S3)}$$

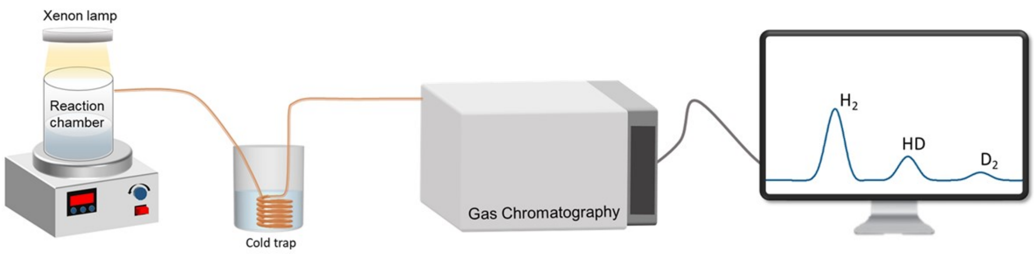

Figure S1. Schematic diagram of catalytic separation experiment

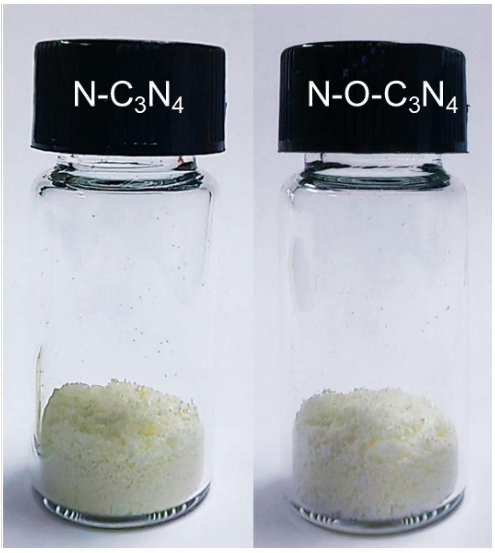

Figure S2. Physical digital photos of N-C_3N_4 and N-O-C_3N_4.

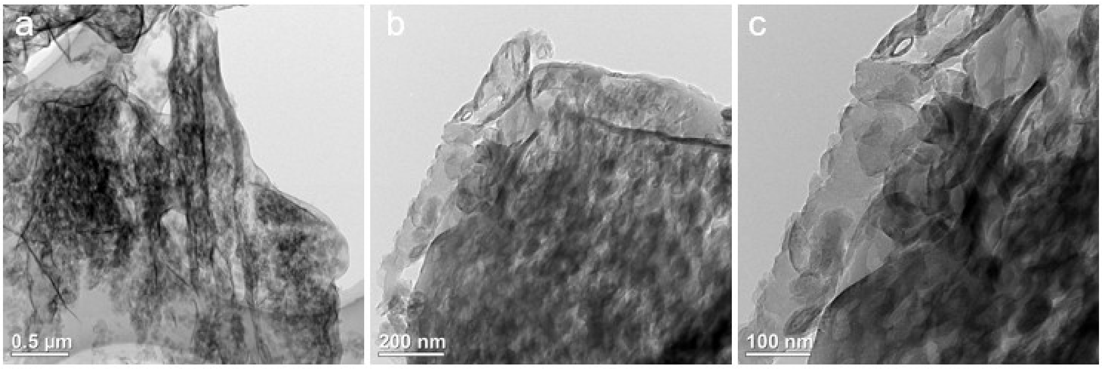

Figure S3. The TEM images of N-C_3N_4.

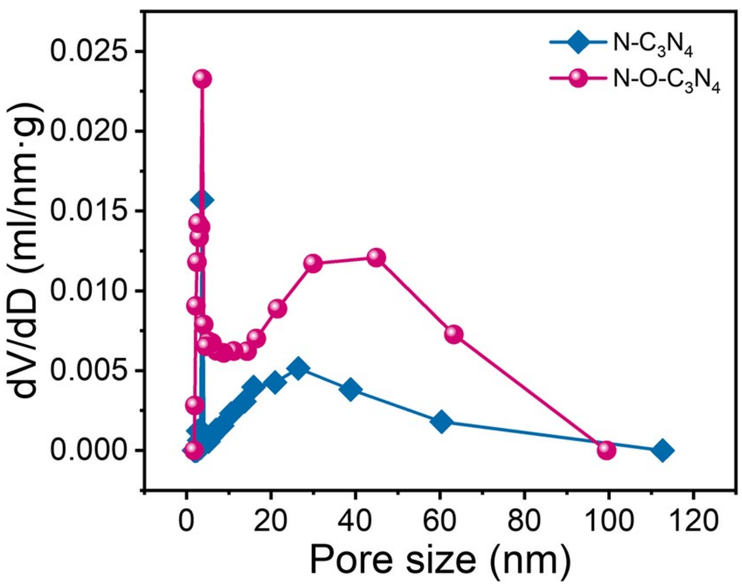

Figure S4. The pore volume distribution of N-C_3N_4 and N-O-C_3N_4.

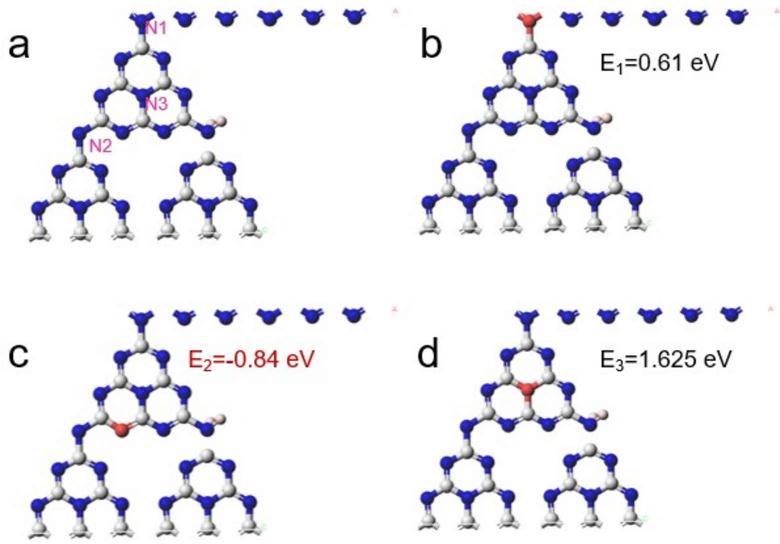

Figure S5 The formation energy of O-doped unit structures at different positions was calculated.

About the unit structure of O-doing in different position; The formation energy was calculated through overall reaction energy by the below function:

$$E_f = E_{total(N,O)} + E_N - E_{total(N)} - E_O$$

Where E_f is overall reaction energy, $E_{total(N,O)}$ is the overall bond energy of unit structure of different units, $E_{total(N)}$ is the overall bond energy of unit structure of N doping units, E_N, E_O is the corresponding bond energy. The formation energies of N1 and N3 sites are both positive, so it is not suitable for doping O atoms. The stability of N-O-CNNS unit structures was assessed in terms of the overall reaction energy (**−0.84 eV**) and edge (N2) was much more favorable than other positions.

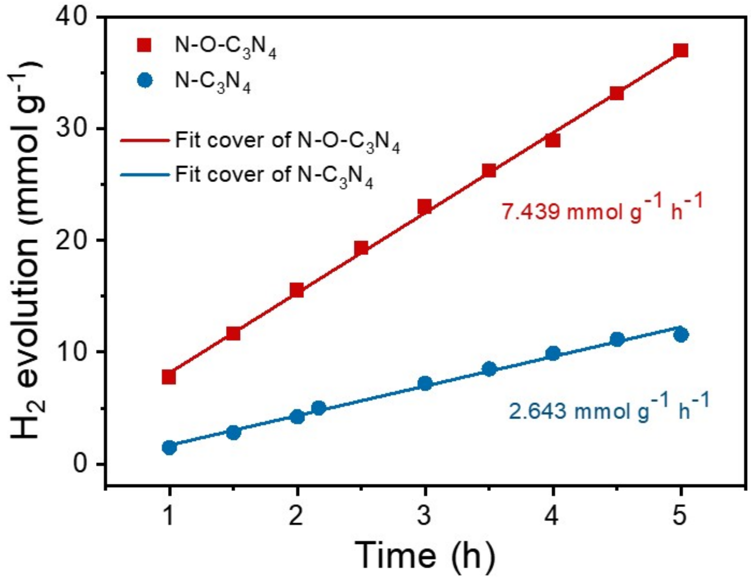

Figure S6. The hydrogen production rate of N-C_3N_4 and N-O-C_3N_4 in the photolysis of pure water under visible light conditions.

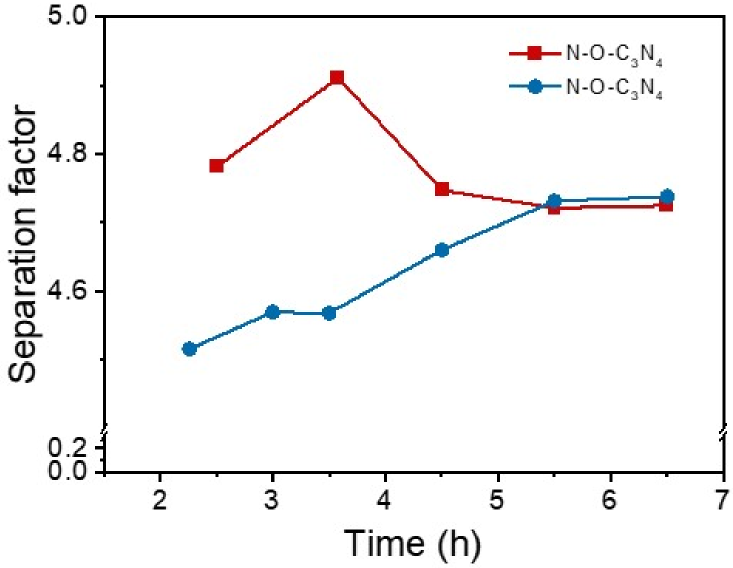

Figure S7. Separation coefficients of N-C_3N_4 and N-O-C_3N_4.

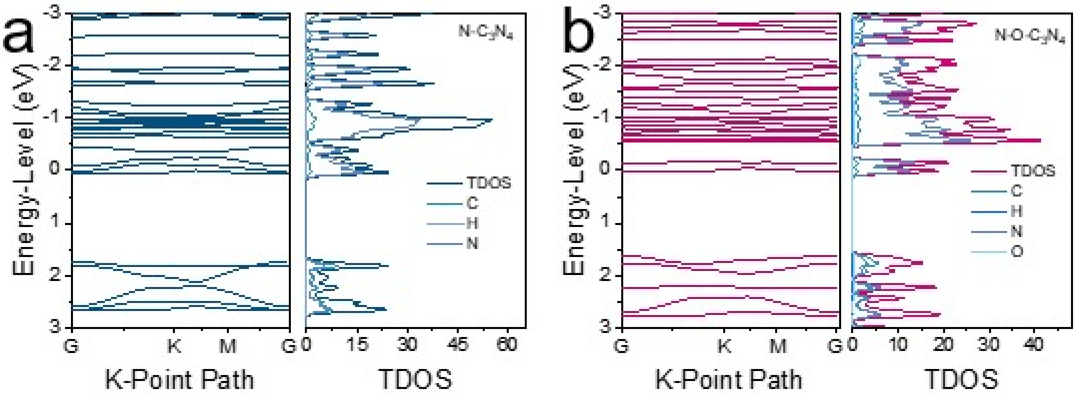

Figure S8. The Band structures and corresponding DOS diagram of (a) N-C_3N_4 and (b)N-O-C_3N_4.

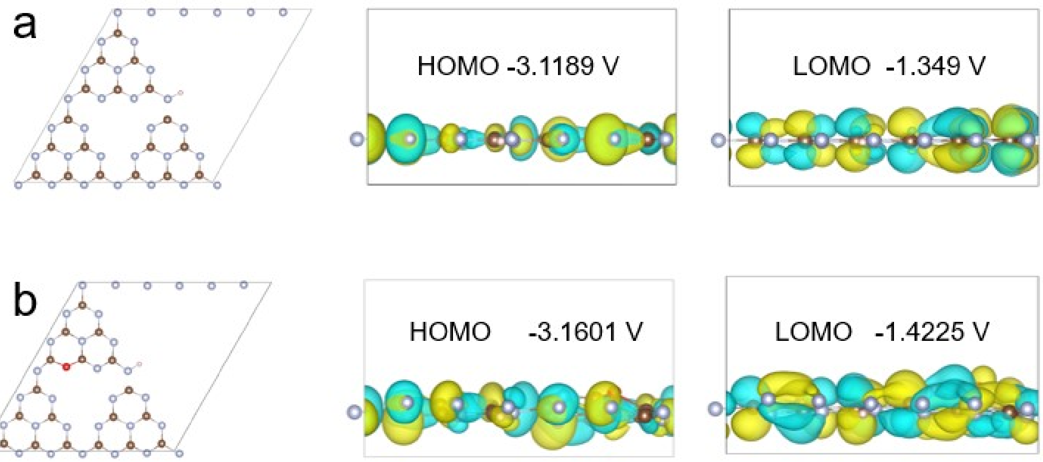

Figure S9. The model structures of (a) N-C_3N_4 and (b)N-O-C_3N_4, and their corresponding LOMO and HOMO orbitals.

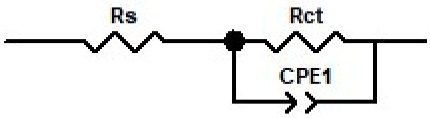

Figure S10. The simplified equivalent circuit model of Pt-based electrodes.

Table S1 Elemental contents of $N\text{-}C_3N_4$ and $N\text{-}O\text{-}C_3N_4$.

	C (at %)	N (at %)	O (at %)
$N\text{-}O\text{-}C_3N_4$	44.6	48.7	**6.7**
$N\text{-}C_3N_4$	45.7	49.0	**5.3**

Table S2 Rs and Rct of $N\text{-}C_3N_4$ and $N\text{-}O\text{-}C_3N_4$ when catalyzing HER and DER

Samples	$N\text{-}O\text{-}C_3N_4$-HER	$N\text{-}C_3N_4$-HER	$N\text{-}C_3N_4$-DER	$N\text{-}O\text{-}C_3N_4$-DER
Rs (Ω)	19.597	21.391	21.391	19.609
Rct (Ω)	38.776	60.77	338.29	383.7

Table S3 Comparison of hydrogen isotope separation applications.

Number	Sample	Separation method	Separation factor	Test method	Ref.
1	GO/PG/GO membrane	Membrane separation	the selectivity of H_2O/D_2O is ≈35.2	NMR- 1H spectroscopy	[1]
2	NF/Gr-decorated Pt	Membrane separation	7.27 ± 0.10	Liquid water isotope analyzer	[2]
3	NF-decorated Pt		6.31 ± 0.03		
4	NF/Gr/NF-coated Pt		4.33 ± 0.03		
5	NF-coated Pt		3.99 ± 0.03		
6	NF/Gr		1.15		
7	NF/Gr/NF		1.08		
8	polymer electrolyte membrane water electrolysis (PEMWE)	Water electrolysis	2.0-3.0	Mass spectrometer	[3]
9	CVD-graphene devices	Water electrolysis	≈10	Mass spectrometry	[4]
10	MoS_2-RS	Water electrolysis	10.22 6.33 for the commercial Pt/C catalyst	Mass spectrometry	[5]
11	CVD graphene	Water electrolysis	~ 8	Mass spectrometry measurements	[6]
12	NiP_2/C	Water electrolysis	6.36	Gas chromatograph	[7]
13	Pt-N_2C_2	Water electrolysis	6.83	Gas chromatography	[8]
14	Au/C	Water electrolysis	7.47	Liquid water isotope analyzer	[9]
15	Cu-based porous coordination polymer	Filtering and Separation	2.3	Temperature-programmed desorption spectra	[10]
16	alkaline membrane fuel cell (AMFC) with a Pt catalyst	Polymer electrolyte fuel cells	1.64	Electrochemical	[11]
17	Metal–organic frameworks	Kinetics-based vapour separation	210	Temperature-programmed desorption spectra	[12]
18	$Cd_{0.5}Zn_{0.5}S(OH)$-SH	Full-spectrum illumination photocatalysis	11	Mass spectrometry	[13]
19	**N-O-C_3N_4**	**Visible-light**	**6.44**	**Gas chromatography**	**This**

photocatalysis	work

[1] Liang J., Zhang X., Liu T.Q., Gao X.D., Liang W.B., Qi W., Qian L.J., Li Z., Chen X.M., Macroscopic Heterostructure Membrane of Graphene Oxide/Porous Graphene/Graphene Oxide for Selective Separation of Deuterium Water from Natural Water. Advanced materials 2022 34 e2206524.
[2] Xue X., Chu X., Zhang M., Wei F., Liang C., Liang J., Li J., Cheng W., Deng K., Liu W., High Hydrogen Isotope Separation Efficiency: Graphene or Catalyst? ACS applied materials & interfaces 2022 14 32360-32368.
[3] Harada K., Tanii R., Matsushima H., Ueda M., Sato K., Haneda T., Effects of water transport on deuterium isotope separation during polymer electrolyte membrane water electrolysis. International Journal of Hydrogen Energy 2020 45 31389-31395.
[4] M. Lozada-Hidalgo S.H., O. Marshall,A. Mishchenko, A. N. Grigorenko,, R. A. W. Dryfe B.R., I. V. Grigorieva, A. K. Geim, Sieving hydrogen isotopes through two-dimensional crystals. Science 2016 351.
[5] Zhao Q., Pang M., Tang C., Xiang X., Wang X., Chen J., Chen C., Molybdenum disulfide nanosheets rich in edge sites for efficient hydrogen isotope separation by water electrolysis. Electrochimica Acta 2023 464 142780.
[6] Lozada-Hidalgo M., Zhang S., Hu S., Esfandiar A., Grigorieva I.V., Geim A.K., Scalable and efficient separation of hydrogen isotopes using graphene-based electrochemical pumping. Nature communications 2017 8 15215.
[7] Hu C., Ding F., Lv C., Zhou L., Zeng N., Liu A., Cai J., Tang T., NiP2 as an efficient non-noble metal cathode catalyst for enhanced hydrogen isotope separation in proton exchange membrane water electrolysis. Separation and Purification Technology 2025 352 128249.
[8] Xu J., Li R., Yan X., Zhao Q., Zeng R., Ba J., Pan Q., Xiang X., Meng D., Platinum single atom catalysts for hydrogen isotope separation during hydrogen evolution reaction. Nano Research 2022 15 3952-3958.
[9] Xue X., Zhang M., Wei F., Liang C., Liang J., Li J., Cheng W., Deng K., Liu W., Gold as an efficient hydrogen isotope separation catalyst in proton exchange membrane water electrolysis. International Journal of Hydrogen Energy 2022 47 26842-26849.
[10] Krause S., Active Separation of Water Isotopologues by Local Molecular Motion in Microporous Framework Materials. Angew. Chem. Int. Ed. 2023.
[11] Ogawa R., Matsushima H., Ueda M., Hydrogen isotope separation with an alkaline membrane fuel cell. Electrochemistry Communications 2016 70 5-7.
[12] Su Y., Otake K.I., Zheng J.J., Horike S., Kitagawa S., Gu C., Separating water isotopologues using diffusion-regulatory porous materials. Nature 2022 611 289-294.

[13]Feng X., Zang Q., Feng X., Lv B., Yu H., Sun T., Yuan Z., Liu J., Yang Y., Zhang F., Enhanced Solar-to-Hydrogen Conversion and Hydrogen Isotope Separation through Interfacial Hydrogen-Bond Engineering and Homolytic O–H Cleavage on Multianionic Sulfides in Large-Scale Floating Nanocomposites. ACS Catalysis 2024 14 9077-9092.